Compact antenna design and analysis for collision avoidance radar at 76GHz

Eddy Jehamy, Michel Ney, Gabrielle Landrac, Sandrick Le Maguer

▶ **To cite this version:**

Eddy Jehamy, Michel Ney, Gabrielle Landrac, Sandrick Le Maguer. Compact antenna design and analysis for collision avoidance radar at 76GHz. International symposium on antenna technology and applied electromagnetics ANTEM, Jul 2004, Ottawa, Canada. 10.1109/ANTEM.2004.7860657 . hal-02399815

HAL Id: hal-02399815
https://hal.science/hal-02399815

Submitted on 8 Jun 2022

HAL is a multi-disciplinary open access archive for the deposit and dissemination of scientific research documents, whether they are published or not. The documents may come from teaching and research institutions in France or abroad, or from public or private research centers.

L'archive ouverte pluridisciplinaire **HAL**, est destinée au dépôt et à la diffusion de documents scientifiques de niveau recherche, publiés ou non, émanant des établissements d'enseignement et de recherche français ou étrangers, des laboratoires publics ou privés.

Distributed under a Creative Commons Attribution - NonCommercial 4.0 International License

COMPACT ANTENNA DESIGN AND ANALYSIS FOR COLLISION AVOIDANCE RADAR AT 76 GHZ

E. Jehamy, M. M. Ney, G. Landrac, S. Le Maguer

Laboratory of Electronics and Systems for Telecommunications (LEST)
CS 83818, 29238 BREST Cedex 3, FRANCE
Eddy.Jehamy@enst-bretagne.fr

ABSTRACT

Collision avoidance radar systems will become standard equipment on vehicles in the near future. Their purpose is to adjust the distance between vehicles and/or alert the driver when dangerous situations arise. Usually located behind the front bumper, these systems need a compact antenna with high gain, to achieve a long-range detection at 76 GHz. As specifications require high gain, electrically large focusing elements are required. Therefore, the design technique proposed is based on Geometrical Optics (GO). Radiation field patterns of various proposed structures are compared to other techniques such as Method of Moments (MoM), Physical Optics (PO) and measurement. It is found that GO gives some reasonably good results for a fast design.

INTRODUCTION

Future collision avoidance radars have specifications that are defined as follows [1]:

- Long range detection: 100-150m
- Short-range detection: ±15° angle of view
- Frequency range operation: 76-77 GHz.
- Polarization: Vertical

These characteristics imposes for the antenna a 20-30 dB gain and a detection field of view around ±8° of. Also, side lobes levels should remain below - 20 dB, although - 25 dB is preferred to further lower the false detection rate. In particular, low side lobe levels are required to reduce the potential detection of targets with large radar cross section such as trucks in adjacent lanes. Such situation may cause the system to lock on the vehicle aside the target rather than passing it.

The radar system proposed here uses a monopulse amplitude detection and a FMCW modulation to detect the angular position, and the speed of the obstacles. Other requirements are minimum weight maximum compactness and low cost manufacturing for mass production. This is the reason why structured presented here are based on foam technology. This dielectric material has (imid polymethacrylic) exhibits low-loss (loss-factor $< 10^{-3}$ up to 110 GHz) and a relative permittivity close to unity. Metallic motives can be deposited on the surface and it can be easily machined or conformed by heat pressing [2]. Finally, it is a very low-cost material.

CONSTRAINED METAL PLATE LENS

The first proposed antenna is the constrained metal plate lens. It consists of stacked parallel-plate waveguides. Each plays the role to increase the phase velocity of the wave propagating though, unlike the usual dielectric lens. Thus, the equivalent local refractive index is less than one and given by [3]:

$$n = \sqrt{1 - \left(\frac{\lambda}{2\, d\, \sqrt{\varepsilon_r}} \right)^2} \qquad (1)$$

where d is the distance between plates, λ the free space wavelength and ε_r the parallel-plate medium relative permittivity. Such structures refer to artificial lenses. The electric field vector coming from a primary source should be transverse and parallel to the plates (fig. 1). These are separated by a distance e which should be larger than one half wavelength, and smaller than one wavelength. This condition is required for single mode TE_1 operation.

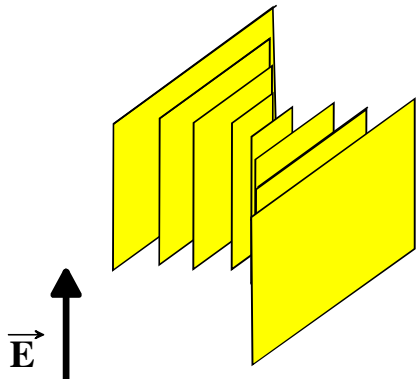

Fig. 1: Structure of an artificial lens

An appropriate plate profile transforms an incident spherical wave to a plane wave at the output side. The proposed design procedure is based on Geometrical Optics (GO). The condition is to enforce the same path length between the rays passing through the different

parallel-plate waveguides. The procedure yields the inner and the outer profile of the lens.

In this paper one considers the case of a trifocal lens that can provide detection with a large angle of view for future radar generation. Indeed, this lens can work as a long-range radar that detects around 0° (broadside), and a short-range radar that can detect around –15° and 15°. Once lens profiles are determined, some optimization is performed by adjusting the focal distance F, the horizontal diameter (D_h) that fixes the number of metal plates, and the vertical diameter (D_v). An optimal pyramidal horn (6.8x5x13mm) was chosen as a primary source that provides a tapered illumination in front of the lens. This can be done by analyzing the near field chart of the horn before inserting the lens (fig. 2). This condition of illumination is important to avoid high side lobe levels.

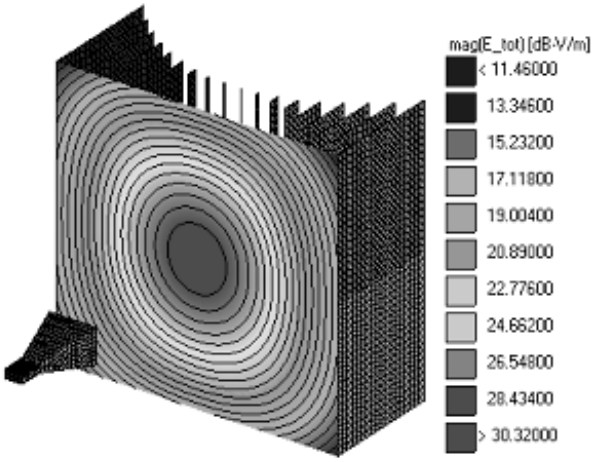

Fig 2: Illumination of the lens by a pyramidal horn

Finally, the optimization procedure yields the following lens' parameters: F = 32mm, D_v = 40mm and D_h = 40.8mm.

Far Field Study and Analysis for the Metal Plate Lens

Investigation will focus on the far field pattern in the horizontal plane (H-plane), because it is the detection plane of the radars. However, E-plane radiation pattern is also important since it should be such as to avoid the detection of fixed obstacles like bridges. Two different models are compared namely, the GO combined with analytical formulas and a full-wave numerical method based on Moment Method (MoM).

In the first model, rays issued from the primary source (horn) assign the amplitude and phase excitation of the illumination at every lens output aperture. Then with Goudet's formula and array theory, the far-field pattern is computed [4]. Hence, based on fig. 3, the total contribution of the N parallel-plate waveguides to the far field is:

$$G_\theta = \left| \sum_{k=1,\,N} S_\theta(k) \right| \qquad (2)$$

where the contribution of the k^{th} element is given by

$$S_\theta(k) = E(k) A_k(\theta)\, \alpha(k) e^{j\varphi(k)} \qquad (3)$$

in which $A_k(\theta)$ is the characteristic function of an open parallel-plate waveguide, E(k) are the amplitude of the waves at the input of the lens k^{th} element coming from the primary source, α(k) is the attenuation of the waves in the element k and φ(k) the phase contribution at the observation point:

$$\varphi(k) = \varphi_{source}^{k} + \frac{2\pi}{\lambda}[n_k \quad (w+ww) - ww \cdot \cos\theta - y(k)\sin\theta] \qquad (4)$$

where φ_{source}^{k} is the phase at the input of the lens k^{th} element coming from the primary source, φ (k) contains also the path length of the waves between the plates (w and ww) and the phase of each wave at the exit of the lens.

Figure 4 shows the H-plane far-field radiation pattern of the optimized lens of fig. 2. As far as the major lobe is

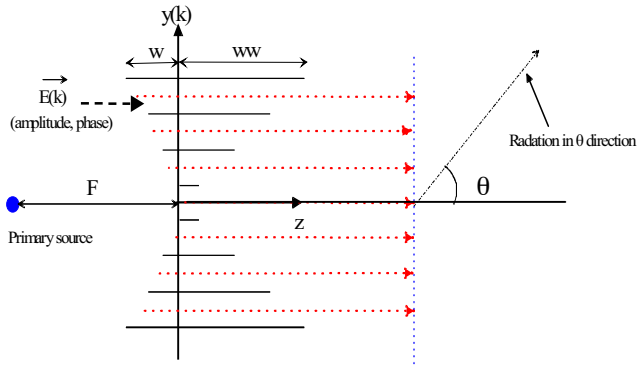

Fig 3: Geometrical parameters for far-field computation by GO

concerned, results match for both methods. However, some significant difference can be observed for side-lobe levels. Clearly, the first approach (GO) is a simplified model which yields negligible computer cost (few seconds) as compared to MoM that requires about half-hour CPU time. Note that the structure has multi-wavelength dimensions. Descrepencies for side-lobe levels are explained by the fact that le GO-based model does not account for diffractions produced by edges

which is the main contribution to side lobe effects. Also note that the interaction between the feeder and the lens has some impact on the first side lobe levels but not at wider angles.

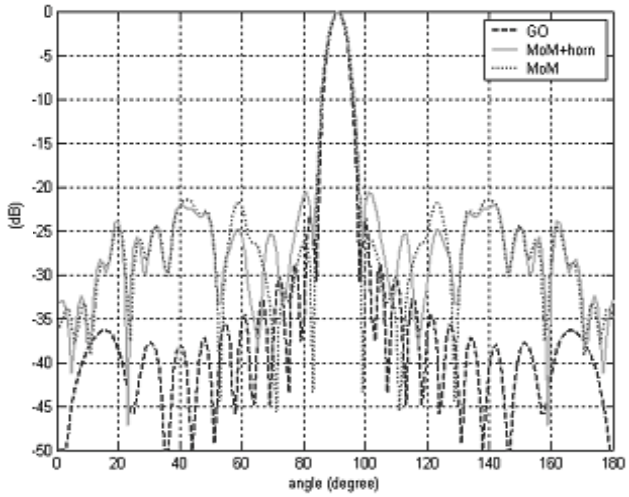

Fig. 4: H-plane radiation pattern: Comparison between different models (antenna illustrated in fig. 2)

Regarding performances of the proposed lens. Simulations show a –22 dB side-lobe rejection and a gain of 22.3 dB. Concerning the compactness we had a structure of: 42x40x40.8 mm. One can anticipate that a planar solution will be more compact. Concerning large angle of view, for radar coverage, the above lens gives good results for a minimum of phase errors.

FRESNEL ZONE LENS ANTENNA

The second type of antenna investigated is the Fresnel zone lens antenna. This antenna is a transmission focusing system which consists of conducting concentric circular strips deposited on a dielectric (fig. 5). To design this lens, GO is also applied that yields the different zone radii:

$$r_n = \sqrt{n\lambda F + \left(\frac{n\lambda}{2}\right)^2} \qquad (5)$$

where n is the n^{th} Fresnel zone radius, F is the focal distance and λ is the wavelength. To realize a more compact structure than the artificial lens, one chooses a focal distance of 20mm with an open-ended waveguide as a feeder. This choice reduces the focal distance, because with a small F, one needs a larger illumination for the lens. If one uses a horn feeder with a small *F* as compared to the lens diameter, one will have larger side-lobe levels as quasi-uniform E field illumination cannot be achieved.

After the optimization of the primary source, one designed a lens including fourteen zones (n=14) with a diameter of 8.64 mm. It was implemented in foam technology as illustrated in fig. 6.

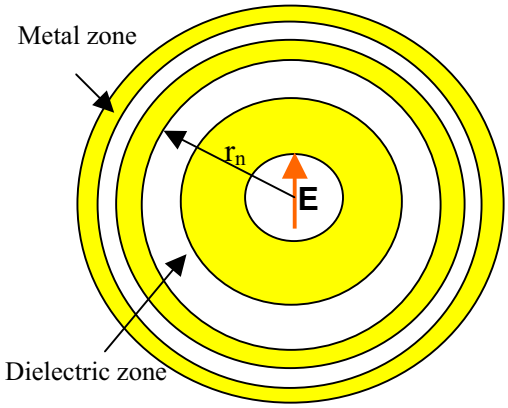

Fig. 5: Front view of a Fresnel zone lens

Fresnel zone far-field H-plane pattern

Physical Optics (PO) and MoM are used and compared in this case. PO takes into account the diffraction and reflection phenomena that occur between conducting strips. However, unlike artificial lens plates, they lie in a

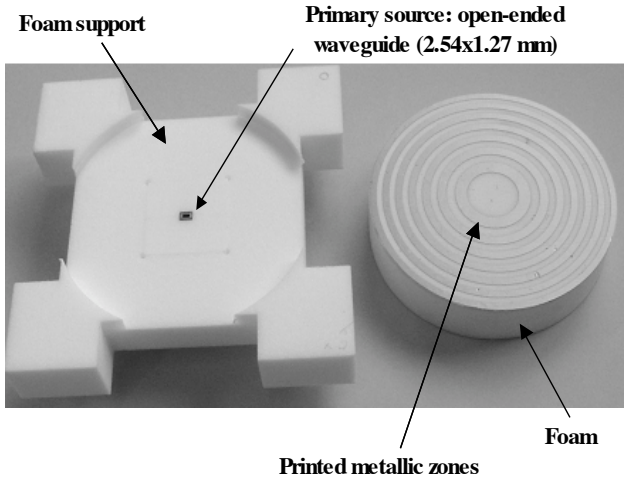

Fig. 6: Photography of the Fresnel zone lens built in foam technology, for measurement

same plane and fewer interactions are expected. This is the reason why PO is more suitable in this case. Figure 7 shows the H-Plane radiation pattern of the Fresnel zone lens computed with both methods. A good match can be observed between both methods. However, some discrepancies occur at grazing angles. Also, one can observe side lobe levels below –22 dB, although, measurements give – 18 dB. Some improvement is still required to achieve some better reduction of side-lobe levels. Finally we can note that for a radar application,

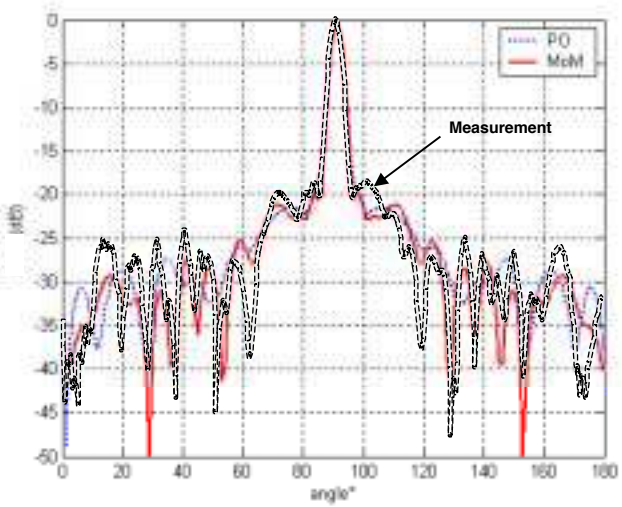

Fig. 7: Fresnel zone lens H-Plane pattern: Comparison between PO, MoM

this lens have a compact structure (86, 4x86, 4x20mm) and good results concerning the side lobes levels (20 dB), and the gain level (24.3 dB, calculated with MoM). To reduce the side lobes levels, we should chose a higher focal distance (F), or a larger number of zones.

Finally, another Fresnel zone lens, also implemented in foam technology, was tested (fig. 8). One can note that the alternate sequence of conducting and dielectric zones is inverted, yielding a "negative" version of the lens illustrated in fig. 6. Also, the frame of the lens is metallized using metallic spraying. It is expected that edge diffraction, source of side-lobe effects, will be reduced. This is confirmed by the results illustrated in fig. 9 where the E-plane radiation pattern is illustrated. One can observe a good match between simulation (MoM) and measurement results. Side-lobe levels below –25 dB and a 24-dB gain are obtained.

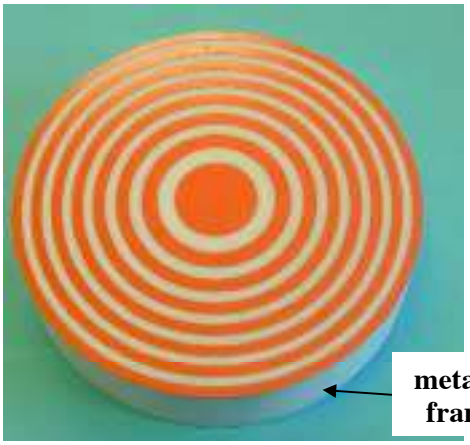

Fig. 8: Fresnel zone lens built in foam technology. "Negative" version of the lens illustrated in fig. 6.

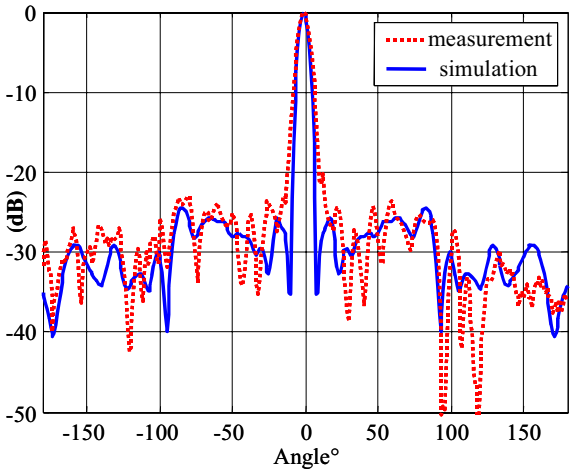

Fig. 9: E-plane radiation pattern (lens of fig. 8): Comparison between simulation (MoM) and measurement.

CONCLUSIONS

Various focusing elements for radar antenna at millimeter-wave frequency were proposed and investigated. Emphases were put on compactness and low-cost technology. Also, specifications for application in future automotive radar generation were considered. Solutions implemented in low-cost foam technology were proposed and investigated. Design approaches based on full-wave analysis (MoM) and asymptotic methods such as GO (fast algorithm) and PO were used and compared with measurement. Results show some reasonably good agreement. Fresnel zone lens yield the best compactness along with performances close to specifications. Other structures are presently under investigation.

REFERENCES

[1] S.W. Alland, “Antenna requirements and architecture tradeoffs for an automotive forward looking radar “, Proc. IEEE Radar Conference, RADARCON'98, Dallas, May 1998 pp.367-72.

[2] F. Gallée, G. Landrac and M.M. Ney, "Artificial Lens for Third-Generation Automotive Radar Antenna at Millimetre-Wave Frequencies", IEE Proceedings, Microwaves, Antennas and Prop., Volume 150, Issue 6, pp. 470-476, Dec. 2003

[3] F. Gallée, G. Landrac and M. M. Ney, "Monopulse millimeter-wave radar antenna with an artificial lens focusing system", Proc. European Workshop on Integrated Radio-Communication Systems, Angers, France, May 2002, pp. 187-190.

[4] C.J. Sletten, "Reflector and Lens Antenna - Analysis and Design Using Pc's; Version 2.0 : software and user's manual " , Artech House, 1991.